Electronic States of TlX (X = As, Sb, Bi): A Configuration Interaction Study

Anjan Chattopadhyay and Kalyan Kumar Das*

Physical Chemistry Section, Department of Chemistry, Jadavpur University, 700 032, India

Received: April 12, 2004; In Final Form: June 18, 2004

Ab initio based relativistic configuration interaction (CI) calculations are carried out to study the electronic spectrum of TlX (X = As, Sb, Bi) molecules. Potential energy curves and spectroscopic constants of low-lying electronic states of these isomers have been computed. Dissociation energies of ground-state molecules are calculated and compared with the experimentally determined values. Effects of the spin−orbit coupling on the spectroscopic properties are studied. The zero-field splitting of the ground state of TlX has been estimated from the spin−orbit CI results. The heavier molecule, TlBi, has a stronger effect of the spin−orbit coupling. Many avoided crossings in the potential curves of Ω states of these isomers are reported. Dipole moments of the ground and lowest few bound states, such as $^3\Pi$,$^1\Sigma^+$, $^1\Delta$, and $^1\Pi$, of TlX have been calculated. Transition probabilities of dipole-allowed and spin-forbidden transitions of these molecules are computed. The radiative lifetimes of some of the excited 0^+ states are also estimated.

I. Introduction

The compounds of group III and V have been well studied in the past several decades because of their technological importance as materials. The spectroscopic properties of diatomic molecules such as GaAs, GaP, InSb, InP, etc. are also known. The clusters of GaAs have been thoroughly studied by Smalley and co-workers[1−6] by using laser-induced photoionization and the time-of-flight mass spectrometry measurement. Lemire et al.[7] have studied the jet-cooled GaAs molecule by the resonant two-photon ionization spectroscopy. The GaX and InX (X = P, As, Sb) molecules are also studied in rare-gas matrixes for their infrared absorption spectrum.[8−10]

In the course of a mass spectrometric study[11] of the Tl−As system, the TlAs molecule was detected and its identification was based on mass, isotropic distribution, intensity shutter profile, and appearance potential (9 ± 1 eV). The dissociation energy of the molecule was obtained by measuring the enthalpy of the reaction $Tl_{(g)} + 1/2As_{2(g)} \rightarrow TlAs_{(g)}$. The molecular parameters used in the calculation of the free energy function of TlAs are $r_e = 2.45$ Å and $\omega_e = 159$ cm^{-1}. The enthalpy of the above reaction has been reported to be -1.0 ± 0.5 kcal mol^{-1}. From these thermodynamic data, the dissociation energy of TlAs is estimated to be 46.4 ± 3.5 kcal mol^{-1}. However, because of the uncertainty in the choice of r_e and ω_e, it is not expected that the reported D_0^0 value will be very accurate. No electronic transitions have been detected so far for the TlAs molecule.

The dissociation energy of the next heavier TlSb molecule in the gas phase has also been determined from thermodynamic data. The reported D_0^0 value of TlSb from such thermodynamic studies[12,13] is 1.31 ± 0.11 eV. The electronic spectrum of the TlSb molecule has also not been known before, either experimentally or theoretically.

The TlBi molecule in the series has been identified in the gas phase by the Knudsen cell-mass spectrometric technique.[14] Since the molecule is isosteric with Pb_2, one may expect some similarity in their spectral properties. Assuming the equilibrium bond length of 2.72 Å and vibrational frequency of 118 cm^{-1} for the ground state of the TlBi molecule, the thermodynamic treatment of the mass spectrometric data has led to the value of the dissociation energy D_0^0 (TlBi) = 1.21 ± 0.13 eV. Like TlAs and TlSb, the electronic spectrum of the TlBi molecule has not been studied so far.

In recent years, the phosphide, arsenide, antimonide, and bismuthide molecules of gallium and indium have been theoretically studied by large-scale configuration interaction (CI) calculations.[15−22] However, similar diatomic molecules of thallium have not been studied at all. In this paper, for the first time, we report the electronic structure and spectroscopic properties of TlX (X = As, Sb, Bi) molecules. Potential energy curves of low-lying states and spectroscopic constants of bound states with and without spin−orbit coupling are computed for these molecules. Since the TlBi molecule is rather heavy, the spin−orbit coupling is expected to change its spectral features to a larger extent than the lighter isomers. The calculated results for these molecules are also compared.

II. Computational Details

The semi-core type relativistic effective core potentials (RECP) of the thallium atom have been taken from Wildman et al.,[23] keeping $5d^{10}6s^26p^1$ electrons in the valence space. Therefore, 68 core electrons are replaced by these pseudo potentials. Similarly, $3d^{10}4s^24p^3$ electrons of As are retained in the valence space, while the remaining inner electrons are substituted by the semi-core pseudopotentials of Hurley et al.[24] For the Sb atom, the $4d^{10}5s^25p^3$ electrons of Sb are kept in the valence space and the inner electrons are replaced by similar RECP of LaJohn et al.[25] The semi-core RECP, which retain $5d^{10}6s^26p^3$ electrons of the Bi atom in the valence space, are taken from Wildman et al.[23] Therefore, for all three isomers, 28 electrons remain active in the valence space for self-consistent field (SCF) and CI calculations.

The Gaussian basis set of the type (4s5p5d1f) for the thallium atom is taken from Wildman et al.[23] without any contraction. The basis set is compatible with the corresponding RECP used in the calculation. The (3s3p4d) basis set of Hurley et al.[24] for

* Corresponding author. E-mail: ju_daskalyan@hotmail.com; das_kalyank@yahoo.com.

10.1021/jp048398z CCC: $27.50
Published on Web 08/07/2004

As is augmented with some diffuse functions. A set of s and p functions with exponents 0.012 and 0.015 a_0^{-2}, respectively, has been added to the above-mentioned basis set of As. These exponents have been taken from the previous work of Alekseyev et al.[26] In addition, a set of f functions with an exponent of 0.44 a_0^{-2} is included so that the final basis set of As becomes (4s4p4d1f). The exponent of the f functions is obtained by optimizing the ground-state energy of the arsenic atom at the CI level. For the antimony atom, the (3s3p4d) basis set of LaJohn et al.[25] has been augmented with two s functions of exponents 0.07 and 0.013 a_0^{-2}, and two sets of p functions of exponents 0.03 and 0.01 a_0^{-2}, which are taken from Alekseyev et al.[27] Two sets of diffuse d functions of exponents 0.1305 and 0.0534 a_0^{-2}, and a set of f functions of exponent 0.46 a_0^{-2} from Balasubramanian[28] have been included in the basis set. However, first two d functions are contracted so that the final basis set of Sb becomes (5s5p6d1f)/[5s5p5d1f].

The (6s6p6d) basis functions of Bi as reported by Wildman et al.[23] are contracted to (4s4p4d). A set of f functions with the exponent of 0.30 a_0^{-2} has been added to this basis. The exponent was optimized by Lingott et al.[29] at the CI level of treatment for the ^{2}D excited atomic state of the Bi atom. Therefore, the final basis set of Bi employed in the calculation of TlBi is (6s6p6d)/[4s4p4d1f].

SCF calculations are carried out for the $(\pi^2)^3\Sigma^-$ state of all three TlX (X=As, Sb, Bi) molecules with 28 valence electrons. All the calculations are performed in the C_{2v} subgroup of the $C_{\infty v}$ main group keeping Tl at the origin and X in the $+z$ axis. Since the $5d^{10}$ and nd^{10} (n = 3,4,5) electrons of Tl and X, respectively, do not participate much in the bonding, these 20 d electrons are kept frozen in the CI steps. Therefore, only eight electrons are used to obtain the excited configurations used in the multireference singles and doubles configuration interaction (MRDCI) codes of Buenker and co-workers.[30−35] Some of the SCF MOs are localized d orbitals of the constituting atoms, while there are orbitals of very high orbital energies which are discarded. Finally, the number of active orbitals for CI calculations are (37, 20, 20, 7), (43, 22, 22, 9), and (41, 21, 21, 8) for TlAs, TlSb, and TlBi molecules, respectively. The numbers in parentheses refer to A_1, B_1, B_2, and A_2 symmetry orbitals. A configuration-selection threshold has been kept at 1.5 μhartrees for TlAs, while for TlSb and TlBi, it is fixed at 2.0 μhartrees. Although the total number of configuration state functions generated is large, the final number of secular equations to be solved remains below 50 000. The energy extrapolation technique and Davidson's correction[35,36] are employed to estimate the full CI energy. The sum of the squares of CI coefficients of the reference configurations lies in the range 0.93−0.95, which should provide fairly accurate energies and wave functions.

The spin−orbit operators of thallium and bismuth atoms as derived from the corresponding RECP are taken from Wildman et al.,[23] while those of As and Sb are taken from Hurley et al.[24] and La John et al.,[25] respectively. For each of three TlX molecules, the spin−orbit coupling has been introduced by a two-step method, as discussed elsewhere.[38] The spin−orbit calculations have been carried out in the C_{2v}[2] symmetry double group, and 0^+, 0^-, 1, 2, 3, 4 components are present in A_1, A_2, and B_1/B_2 irreducible representations. The size of these three blocks remains within 50. All states correlating with the lowest two dissociation limits, such as ^{2}P(Tl)+^{4}S(X) and ^{2}P(Tl)+^{2}D(X), are allowed to mix through the spin−orbit coupling. The potential energy curves are fitted into polynomials which are used to solve the numerical Schrödinger equations.[39] The transition moments for the pair of vibrational functions involved in a particular transition are computed. The spontaneous emission coefficients, and hence, transition probabilities, are calculated subsequently. The radiative lifetimes of the excited states at different vibrational levels have been computed from the respective transition probability data.

TABLE 1: Relative Energies (cm^{-1}) of TlX in the Second Dissociation Limit

	relative energy of Tl(^{2}P)+X(^{2}D)	
X	exptl[a]	calcd
As	10 794	12 951
Sb	9351	10 942
Bi	13 931	10 183

[a] Reference 40.

TABLE 2: Spectroscopic Constants of Low-Lying Λ-S States of TlAs

state	T_e/cm^{-1}	r_e/Å	ω_e/cm^{-1}	state	T_e/cm^{-1}	r_e/Å	ω_e/cm^{-1}
$X^3\Sigma^-$	0	2.84	154	$3^1\Sigma^+$	28 305	3.60	73
$^3\Pi$	2482	2.63	170	$2^5\Sigma^-$	29 355	3.13	86
$^1\Pi$	7675	2.58	188	$2^5\Pi$	37 938	3.05	99
$^1\Delta$	7829	2.81	161	$3^5\Sigma^-$	38 557	3.29	72
$^1\Sigma^+$	9467	2.61	151	$3^5\Pi$	42 620	3.23	82
$2^1\Sigma^+$	15 583	2.66	202	$^5\Sigma^+$	44 467	2.73	153
$2^3\Pi$	16 349	3.33	99	$2^5\Sigma^+$	50 933	2.73	165
$A^3\Pi$	22 554	3.09	79	$^5\Delta$	51 841	2.65	176
$2^1\Pi$	23 649	3.24	59				

III. Potential Energy Curves and Spectroscopic Properties of Λ-S States

Like all other group III−V molecules, the ground states of Tl(^{2}P) and X(^{4}S) atoms correlate with four Λ-S molecular states of $^3\Sigma^-$, $^3\Pi$, $^5\Sigma^-$, and $^5\Pi$ symmetries. The ground-state symmetry of each of these molecules is $X^3\Sigma^-$. The first excited state (^{2}D) of the X atom combines with the ground state of thallium to generate 18 singlet and triplet states of Σ, Π, Δ, and Φ symmetries. The relative energies of the second dissociation limit Tl(^{2}P) + X(^{2}D) with respect to the lowest one are calculated from the molecular calculations at a very large bond distance. The comparison with the observed data from the atomic spectral study is shown in Table 1. A discrepancy of 1500−3700 cm^{-1} is due to the absence of the spin−orbit coupling in the Λ-S CI calculations. The spin−orbit interactions in TlAs and TlSb are comparatively less than those in TlBi. The computed relative energy of the second limit is, however, overestimated both for TlAs and TlSb, while it is underestimated by more than 3700 cm^{-1} for the heavier TlBi molecule.

A. TlAs. In Table 2, the computed spectroscopic constants of 17 Λ-S states of the TlAs molecule within 6.5 eV of energy are tabulated. The ground state ($X^3\Sigma^-$) of the molecule has an equilibrium bond length of 2.84 Å with ω_e = 154 cm^{-1}. Although experimental results are not yet available, it is expected that the actual r_e would be around 2.80 Å, while the observed ω_e would be somewhat larger than 154 cm^{-1}. The dominant configuration describing the ground state of TlAs is the same as that of other group III−V molecules. The MRDCI estimated dissociation energy (D_e) of the ground state of TlAs is about 1.42 eV, which is considerably smaller than the thermodynamically[11] determined D_0^0 value of 2.01 ± 0.15 eV which assumes r_e = 2.45 Å and ω_e = 159 cm^{-1}. However, the MRDCI method is known to underestimate the dissociation energy by 0.3−0.6 eV because of the use of effective core potentials, basis set limitation, absence of d correlation, and spin−orbit coupling.

Potential energy curves of low-lying states of TlAs up to 50 000 cm^{-1} are given in Figure 1a,b. The first excited state of

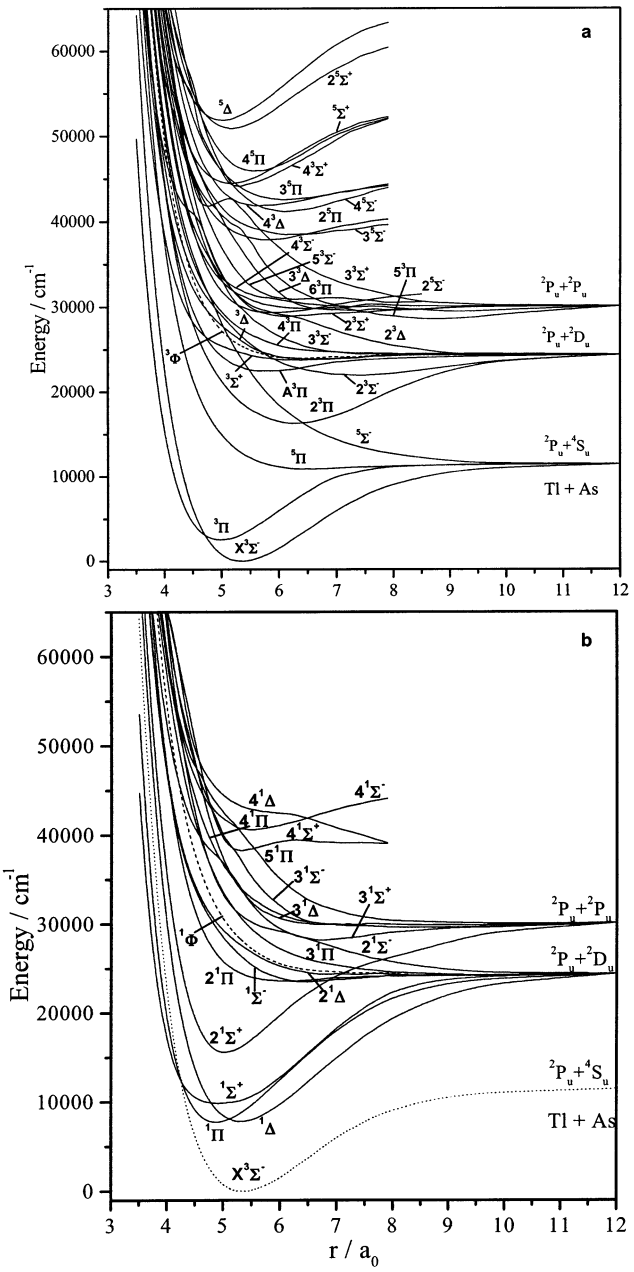

Figure 1. Computed potential energy curves of low-lying (a) triplet and quintet (b) singlet Λ-S states of TlAs.

the $^3\Pi$ symmetry has a shorter bond length and longer vibrational frequency than those of the ground state. The state lies only 2482 cm^{-1} above the ground state. The singlet counterpart of the $^3\Pi$ state has even a shorter bond length, and the computed singlet−triplet splitting [$\Delta E(^1\Pi - {}^3\Pi)$] is about 5193 cm^{-1}. Both these Π states originate from the same $\sigma' \rightarrow \pi$ excitation. Another configuration arising from the $\sigma' \rightarrow \pi^*$ excitation also contributes to these states. Two singlets, such as $^1\Delta$ and $^1\Sigma^+$, arising out of the ground-state configuration are next in the energy order. The $^1\Delta$ and $^1\Pi$ states are nearly degenerate, with a gap of less than 200 cm^{-1}. The r_e and ω_e values of $^1\Delta$ are comparable with those of the ground state. The compositions of CI wave functions of $^1\Sigma^+$ and $2^1\Sigma^+$ have shown a strong avoided crossing which forces the $2^1\Sigma^+$ state to dissociate into the second asymptote, Tl(^{2}P) + As(^{2}D). As a result, the vibrational frequency of $2^1\Sigma^+$ is larger than that of $^1\Sigma^+$ by at least 50 cm^{-1}, and the potential energy curve of $^1\Sigma^+$ around r_e looks flattened. The minimum of the adiabatic curve of the $2^1\Sigma^+$ state lies around 15 583 cm^{-1}.

TABLE 3: Spectroscopic Constants of Low-Lying Λ-S States of TlSb

state	T_e/cm^{-1}	r_e/Å	ω_e/cm^{-1}	state	T_e/cm^{-1}	r_e/Å	ω_e/cm^{-1}
$X^3\Sigma^-$	0	3.08	117	$3^1\Sigma^+$	26 289	3.83	60
$^3\Pi$	3230	2.89	129	$2^5\Sigma^-$	29 389	3.38	58
$^1\Delta$	6547	3.05	122	$2^5\Pi$	36 831	3.33	68
$^1\Pi$	7805	2.84	138	$3^5\Sigma^-$	37 251	3.54	53
$^1\Sigma^+$	9357	2.93	108	$3^5\Pi$	42 450	3.64	49
$2^3\Pi$	15 023	3.66	69	$^5\Sigma^+$	43 493	2.96	121
$2^1\Sigma^+$	15 377	2.88	153	$4^5\Pi$	45 041	3.19	111
$2^3\Sigma^-$	20 022	4.34	32	$^5\Delta$	46 423	3.06	105

Like other isovalent group III−V molecules, a broad potential minimum of the $2^3\Pi$ state of TlAs is also obtained due to a strong avoided crossing with the lower $^3\Pi$ state. The estimated transition energy of the $2^3\Pi$ state is about 16 349 cm^{-1}, with a bond length of 3.33 Å and vibrational frequency of 99 cm^{-1}. The excited $2^3\Sigma^-$ state curve is also very shallow, and the computed ω_e is only 51 cm^{-1}. Higher roots of the ground-state symmetry are found to be repulsive. The third root of the $^3\Pi$ symmetry plays an important role for most of the group III−V molecules. However, only for the GaAs molecule, this state has been experimentally observed. Keeping an analogy with GaAs, the $3^3\Pi$ state of TlAs is designated as $A^3\Pi$. As seen in Figure 1a, this state has a very shallow potential well with a computed vibrational frequency of only 79 cm^{-1}. The MRDCI estimated equilibrium bond length of this state is about 3.09 Å. Although $A^3\Pi$ is an important state for its transition to the ground state, the $A^3\Pi \rightarrow X^3\Sigma^-$ transition is not expected to be strong because the upper state is weakly bound. The potential curves of the higher roots of $^3\Pi$, such as $4^3\Pi$, $5^3\Pi$, and $6^3\Pi$, shown in Figure 1a, are repulsive. The second, third, and fourth roots of $^3\Sigma^+$ undergo two avoided crossings around the bond length of 4.6 and 5.1 a_0, respectively. As a result, a small barrier of 0.12 eV appears in the adiabatic potential curve of the $3^3\Sigma^+$ state. The fourth root of the $^3\Sigma^+$ symmetry is found to be very strongly bound at a shorter bond length. However, the near-repulsive or repulsive curves of the second and third root of $^3\Sigma^+$ interact strongly in 4.5−5.0 a_0 region and change the characteristics of the potential curve of the $4^3\Sigma^+$ state. Two singlets, such as $2^1\Pi$ and $3^1\Sigma^+$, are also weakly bound. An avoided curve crossing is noted between the third and fourth root of $^1\Sigma^+$. A shallow minimum in the potential curve of $4^1\Sigma^+$ near 38 000 cm^{-1} is seen in Figure 1b. The higher roots of $^1\Delta$, $^1\Pi$, and $^1\Sigma^-$ symmetries are repulsive.

There is a set of seven quintet states of Σ^+, Σ^-, Π, and Δ symmetries in the energy range 29 000−52 000 cm^{-1}. These states dissociate mostly to the higher asymptotes. Of these, $^5\Sigma^+$, $2^5\Sigma^+$, and $^5\Delta$ states are more strongly bound than others. The computed equilibrium bond lengths of these states are shorter than 3.0 Å. These states have also large ω_e's, which are comparable with those of the low-spin states of the TlAs molecule. For other quintets, the bond lengths are longer than 3.0 Å. Although these quintets are not very important in terms of any electronic transition to the lower-lying states, their spin−orbit components may play an important role in perturbing some of the transitions.

B. TlSb. The computed spectroscopic constants of 15 Λ-S states of the isovalent TlSb molecule are reported in Table 3. The ground state ($X^3\Sigma^-$) of the molecule has a bond length of 3.08 Å and a vibrational frequency of 117 cm^{-1}. The computed dissociation energy (D_e) of the ground state of TlSb is 1.35 eV without the inclusion of any spin−orbit coupling. Incidentally, this is very close to the D_0^0 value of 1.31 ± 0.11 eV derived from the thermodynamic data.[12,13] However, the experimentally determined D_0^0 value of TlSb may not be very accurate because

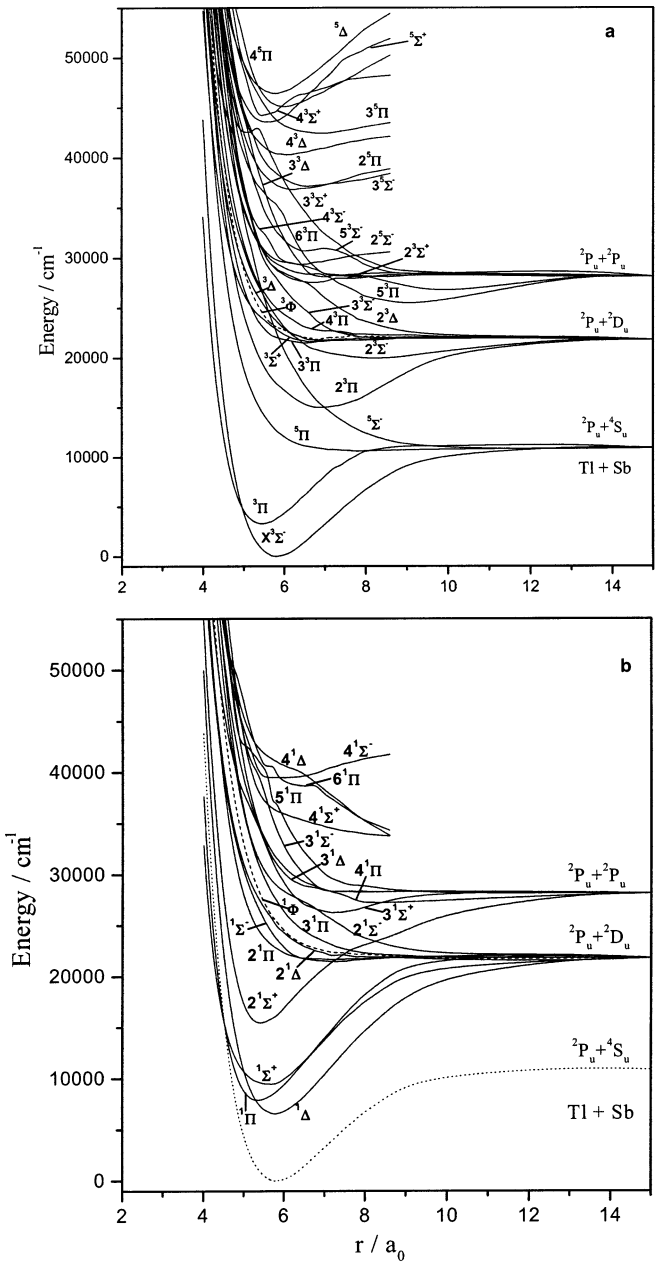

Figure 2. Computed potential energy curves of low-lying (a) triplet and quintet (b) singlet Λ-S states of TlSb.

of the choice of certain parameters required for its determination. On the other hand, the inclusion of the spin−orbit coupling is expected to change D_e to some extent.

The first excited state ($^3\Pi$) lies 3230 cm^{-1} above the ground state with a bond length of 2.89 Å. Potential energy curves of low-lying Λ-S states of TlSb are shown in Figure 2a,b. As expected, both the high-spin low-lying states, such as $^5\Sigma^-$ and $^5\Pi$, are repulsive, and they dissociate into the lowest asymptote. Three singlet states, namely, $^1\Delta$, $^1\Pi$, and $^1\Sigma^+$, lie next to $^3\Pi$ in the energy order. Unlike TlAs, the $^1\Delta$ state of TlSb is more stabilized than $^1\Pi$. The r_e and ω_e values of $^1\Delta$ are comparable with those of the ground state. The energy difference between $^3\Pi$ and $^1\Pi$ states of TlSb is about 4575 cm^{-1}. Both $^3\Pi$ and $^1\Pi$ states originate from the same single excitation $\sigma' \rightarrow \pi$ as in other group III−V molecules. The avoided crossing between the lowest two roots of $^1\Sigma^+$ in the potential energy curves of the TlSb molecule is analogous to that of TlAs. The adiabatic curves are fitted for the estimation of spectroscopic constants of $^1\Sigma^+$ and $2^1\Sigma^+$ states. As a result, the $2^1\Sigma^+$ state has a shorter bond length and larger ω_e than those of $^1\Sigma^+$. The minimum of the adiabatic curve of $^1\Sigma^+$ is located 9357 cm^{-1} above the ground state, while the $2^1\Sigma^+$ state has a transition energy of 15 377 cm^{-1}. The nature of the interaction between these two roots is consistent with their CI wave functions at different bond lengths. The next two higher roots of the $^1\Sigma^+$ symmetry are not strongly bound. In fact, the $4^1\Sigma^+$ state is repulsive, while $3^1\Sigma^+$ has an equilibrium bond length of 3.83 Å with a smaller ω_e value of 60 cm^{-1}.

The characteristics of the $2^3\Pi$ state of TlSb are quite similar to those of TlAs. The shallow minimum of the $2^3\Pi$ state is also due to a strong interaction between the lowest two roots of the $^3\Pi$ symmetry, as noted in TlAs. The fitted adiabatic potential curve of the $2^3\Pi$ state has $r_e = 3.66$ Å and $\omega_e = 69$ cm^{-1}. The $2^3\Pi$ state dissociates into the second asymptote. As noted in Figure 2a, the potential energy curve of $3^3\Pi$ is almost repulsive, converging with the second dissociation limit. The higher excited $^3\Pi$ states, such as $4^3\Pi$, $5^3\Pi$, and $6^3\Pi$, are not bound at all. The upper roots of $^3\Sigma^-$ are not so important from the spectroscopic point of view as the potential curves of $2^3\Sigma^-$, $3^3\Sigma^-$, $4^3\Sigma^-$, and $5^3\Sigma^-$ states are repulsive. Between 29 000 and 43 000 cm^{-1}, there exists a set of four quintets which are weakly bound. However, $^5\Sigma^+$, $4^5\Pi$, and $^5\Delta$ states, which lie beyond 43 000 cm^{-1}, are relatively more strongly bound. The spin−orbit components of these quintets may interact with those of some lower-lying states.

C. TlBi. The computed potential energy curves and spectroscopic parameters of low-lying Λ-S states of the heavier isomer TlBi are reported in Figure 3a,b and Table 4, respectively. The ground state ($X^3\Sigma^-$) of this molecule has an equilibrium bond length of 3.14 Å with $\omega_e = 99$ cm^{-1}. The dominant configuration in the ground-state MRDCI wave function is $...\sigma'^2\pi^2$, where the nature of the molecular orbitals is almost the same as those in other group III−V diatomic molecules. Because of the heavier mass, the electronic spectrum of TlBi is somewhat different than its lighter isomers. The MRDCI estimated ground-state D_e of TlBi is 1.25 eV without any spin−orbit coupling. The thermodynamic treatment of the data from the Knudsen cell-mass spectrometric technique has led to a value of $D_0^0 = 1.21 \pm 0.13$ eV. An excellent agreement with the calculated data seems to be fortuitous as the spin−orbit coupling is expected to be quite large for the TlBi molecule. The experimental $^2P_{3/2}-^2P_{1/2}$ splitting[40] for the Tl atom is 7793 cm^{-1}. The spin−orbit splitting of the first excited state (^{2}D) of Bi is more than 4000 cm^{-1}.

The $^3\Pi$ state lies 2972 cm^{-1} above the ground state with a shorter bond length ($r_e = 2.95$ Å) and larger vibrational frequency ($\omega_e = 110$ cm^{-1}) than those of the ground state. The compositions of the CI wave functions have also confirmed strong avoided crossing of the $^3\Pi$ state curve with its next higher root as in TlAs and TlSb. A shallow minimum in the potential curve of $2^3\Pi$ appears around 3.8 Å with ω_e=56 cm^{-1}. The singlet counterpart of $^3\Pi$ has a transition energy of 7634 cm^{-1} with comparable r_e and ω_e values. The same $\sigma' \rightarrow \pi$ excitation generates both $^3\Pi$ and $^1\Pi$ states. The $^1\Delta$ state originating from the ground-state configuration has a transition energy of 5971 cm^{-1}. The spectroscopic constants of $^1\Delta$ are comparable with those of the ground state. The characteristics of the lowest two roots of the $^1\Sigma^+$ symmetry are also same as those of TlAs and TlSb molecules. As a result, the $2^1\Sigma^+$ state has a shorter bond length and larger ω_e than its lower root ($^1\Sigma^+$). Another curve crossing between the second and third root in the longer bond length region has created a shallow minimum ($r_e = 3.83$ Å) in the potential curve of $3^1\Sigma^+$. As seen in Table 4, there is a set of

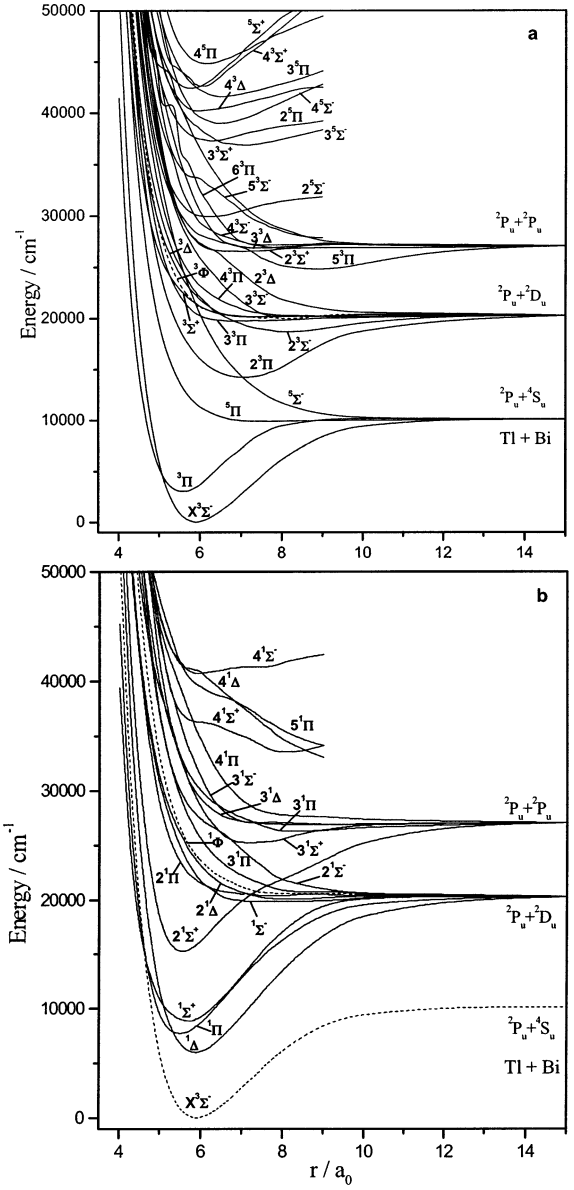

Figure 3. Computed potential energy curves of low-lying (a) triplet and quintet (b) singlet Λ-S states of TlBi.

TABLE 4: Spectroscopic Constants of Low-Lying Λ-S States of TlBi

state	T_e/cm^{-1}	r_e/Å	ω_e/cm^{-1}	state	T_e/cm^{-1}	r_e/Å	ω_e/cm^{-1}
$X^3\Sigma^-$	0	3.14	99	$2^5\Sigma^-$	29 958	3.33	57
$^3\Pi$	2972	2.95	110	$3^5\Sigma^-$	36 884	3.73	45
$^1\Delta$	5971	3.11	105	$2^5\Pi$	37 314	3.32	61
$^1\Pi$	7634	2.91	115	$4^5\Sigma^-$	38 973	3.44	68
$^1\Sigma^+$	8858	2.99	94	$3^5\Pi$	41 610	3.47	59
$2^3\Pi$	14 171	3.80	56	$^5\Sigma^+$	42 364	3.06	102
$2^1\Sigma^+$	15 229	2.94	126	$4^5\Pi$	44 800	3.26	81
$3^1\Sigma^+$	25 189	3.83	50	$5^5\Pi$	48 430	3.30	95

eight quintet states in the range 30 000−48 000 cm^{-1}. Except $^5\Sigma^+$, all quintets are weakly bound and have longer bond lengths correlating with the higher dissociation limits. The $^5\Sigma^+$ state has a bond length even shorter than that of the ground state. Minima of three higher roots of the $^5\Sigma^-$ symmetry are present within 10 000 cm^{-1} of energy. Similarly, $2^5\Pi$, $3^5\Pi$, $4^5\Pi$, and $5^5\Pi$ states are located not very far from each other. The spin−orbit coupling in TlBi is larger than that of the other two isomers; hence, it is expected to affect the calculated results quite significantly.

TABLE 5: Dissociation Correlation between Ω States and the Corresponding Atomic Asymptotes of TlAs

Ω state	atomic states Tl + As	relative energy/cm^{-1} exptl[a]	calcd
0^+, 0^-, 1(2), 2	$^2P_{1/2} + {}^4S_{3/2}$	0	0
0^+(2), 0^-(2), 1(3), 2(2), 3	$^2P_{3/2} + {}^4S_{3/2}$	7793	6870
0^+, 0^-, 1(2), 2	$^2P_{1/2} + {}^2D_{3/2}$	10 593	12 859
0^+, 0^-, 1(2), 2(2), 3	$^2P_{1/2} + {}^2D_{5/2}$	10 915	13 262
0^+, 0^-, 1	$^2P_{1/2} + {}^2P_{1/2}$	18 186	18 769
0^+(2), 0^-(2), 1(3), 2(2), 3	$^2P_{3/2} + {}^2D_{3/2}$	18 386	19 255
0^+, 0^-, 1(2), 2	$^2P_{1/2} + {}^2P_{3/2}$	18 648	19 611
0^+(2), 0^-(2), 1(4), 2(3), 3(2), 4	$^2P_{3/2} + {}^2D_{5/2}$	18 708	19 944

[a] Reference 40.

TABLE 6: Dissociation Correlation between Ω States and the Corresponding Atomic Asymptotes of TlSb

Ω state	atomic states Tl + Sb	relative energy/cm^{-1} exptl[a]	calcd
0^+, 0^-, 1(2), 2	$^2P_{1/2} + {}^4S_{3/2}$	0	0
0^+(2), 0^-(2), 1(3), 2(2), 3	$^2P_{3/2} + {}^4S_{3/2}$	7793	6761
0^+, 0^-, 1(2), 2	$^2P_{1/2} + {}^2D_{3/2}$	8512	10 593
0^+, 0^-, 1(2), 2(2), 3	$^2P_{1/2} + {}^2D_{5/2}$	9854	11 667
0^+(2), 0^-(2), 1(3), 2(2), 3	$^2P_{3/2} + {}^2D_{3/2}$	16 305	16 948
0^+, 0^-, 1	$^2P_{1/2} + {}^2P_{1/2}$	16 396	17 757
0^+(2), 0^-(2), 1(4), 2(3), 3(2), 4	$^2P_{3/2} + {}^2D_{5/2}$	17 647	18 279
0^+, 0^-, 1(2), 2	$^2P_{1/2} + {}^2P_{3/2}$	18 465	19 706

[a] Reference 40.

TABLE 7: Dissociation Correlation between Ω States and the Corresponding Atomic Asymptotes States of TlBi

Ω state	atomic states Tl + Bi	relative energy/cm^{-1} exptl[a]	calcd
0^+, 0^-, 1(2), 2	$^2P_{1/2} + {}^4S_{3/2}$	0	0
0^+(2), 0^-(2), 1(3), 2(2), 3	$^2P_{3/2} + {}^4S_{3/2}$	7793	6595
0^+, 0^-, 1(2), 2	$^2P_{1/2} + {}^2D_{3/2}$	11 419	11 601
0^+, 0^-, 1(2), 2(2), 3	$^2P_{1/2} + {}^2D_{5/2}$	15 438	15 745
0^+(2), 0^-(2), 1(3), 2(2), 3	$^2P_{3/2} + {}^2D_{3/2}$	19 212	18 092
0^+, 0^-, 1	$^2P_{1/2} + {}^2P_{1/2}$	21 661	21 278
0^+(2), 0^-(2), 1(4), 2(3), 3(2), 4	$^2P_{3/2} + {}^2D_{5/2}$	23 231	22 370
0^+, 0^-, 1(2), 2	$^2S_{1/2} + {}^4S_{3/2}$	26 478	
0^+, 0^-, 1(2), 2	$^2P_{3/2} + {}^2P_{1/2}$	29 454	
0^+, 0^-, 1(2), 2	$^2P_{1/2} + {}^2P_{3/2}$	33 165	
0^+(2), 0^-(2), 1(3), 2(2), 3	$^2P_{3/2} + {}^2P_{3/2}$	40 958	

[a] Reference 40.

IV. Spectroscopic Properties of Ω States and Effects of the Spin−Orbit Coupling

For all three TlX (X = As, Sb, Bi) molecules, 34 Λ-S states correlating with the lowest three dissociation limits interact through the spin−orbit coupling. This has generated 74 Ω states that converge to 10 separated atom asymptotes. The relative energies of these asymptotes obtained from the MRDCI calculations of these molecules at a large bond length are compared with the observed values in Tables 5−7. The average $^2P_{3/2}-{}^2P_{1/2}$ splitting for Tl from the MRDCI calculations of TlAs, TlSb, and TlBi is about 6650 cm^{-1}, as compared with the observed value of 7793 cm^{-1}. On the other hand, the agreement between the calculated and observed $^2D_{5/2}-{}^2D_{3/2}$ splitting of As, Sb, and Bi is found to be much better.

A. TlAs. Potential energy curves of some important low-lying states with Ω = 0^+, 0^-, 1, 2, and 3 are shown in Figure 4a−d. The curves show several avoided crossings among the roots of a given symmetry. Table 8 displays the computed spectroscopic constants (T_e, r_e, ω_e, and D_e) of low-lying Ω states of TlAs estimated by fitting the adiabatic potential curves. The zero-field splitting between the components of $X^3\Sigma^-$ is com-

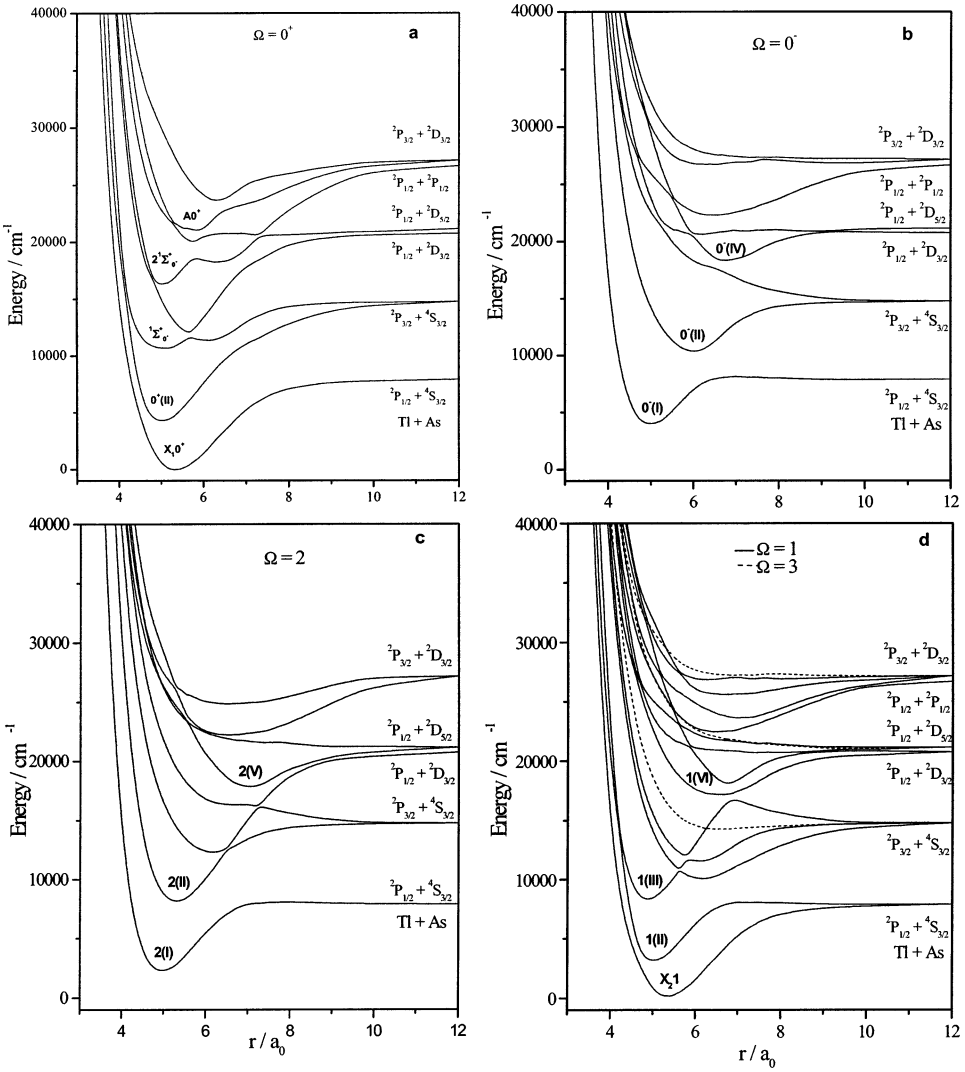

Figure 4. Computed potential energy curves of low-lying Ω states of TlAs for (a) Ω = 0^+, (b) Ω = 0^-, (c) Ω = 2, and (d) Ω = 1, 3.

TABLE 8: Spectroscopic Constants of Low-Lying Ω States of TlAs

state	T_e/cm^{-1}	r_e/Å	ω_e/cm^{-1}	D_e/eV
$X_1 0^+$	0	2.83	142	0.98
$X_2 1$	263	2.84	136	0.94
2(I)	2291	2.63	167	0.70
1(II)	3136	2.66	189	0.59
0^-(I)	3989	2.64	167	0.48
0^+(II)	4220	2.65	182	1.31
2(II)	8204	2.80	158	0.82
1(III)	8345	2.58	188	0.80
0^-(II)	10 440	3.18	120	0.54
$^1\Sigma^+_{0^+}$	10 457	2.65	143	0.53
$2^1\Sigma^+_{0^+}$	16 286	2.65	205	0.61
2(V)	17 964	3.71	96	0.40
0^-(IV)	18 659	3.59	108	0.26
$A0^+$	21 144	3.07	120	0.75

puted to be 263 cm^{-1}, with the $X_1 0^+$ component lying below $X_2 1$. Spectroscopic constants of these two spin components are not much different from those of $X^3\Sigma^-$. In general, the mixing among the spin components is not very large in the Franck−Condon region. Around the equilibrium bond distance, the $X_1 0^+$ component of TlAs is almost pure $X^3\Sigma^-$, while in the shorter bond length region, the $^3\Pi_{0^+}$ component dominates. The contribution of the $^5\Pi_{0^+}$ component increases with the bond length. Four spin components of $^3\Pi$, which split in the inverted order, are denoted as 2(I), 1(II), 0^-(I), and 0^+(II). In the shorter bond length region, 1(II) and 0^+(II) components have a dominant $X^3\Sigma^-$ character, while two other components, such as 2(I) and 0^-(I), remain almost pure $^3\Pi$. However, in the longer bond length region, the extent of mixing of different components is significantly larger. The largest spin−orbit splitting for $^3\Pi$ is nearly 2000 cm^{-1}. Spectroscopic parameters of these four components remain more or less unchanged. The adiabatic curve of the third 0^+ root shows a double minima. In the short-distant minimum. the $^1\Sigma^+$ state dominates and, hence, is denoted as $^1\Sigma^+_{0^+}$, while the long-distant minimum is very shallow. The spectroscopic constants of $^1\Sigma^+_{0^+}$ remain almost unchanged as it is less perturbed by any nearby component. The fifth root of the 0^+ symmetry originates mainly from $2^1\Sigma^+$ in the equilibrium region of the curve. In the energy region of 21 000 cm^{-1}, the mixing of sixth and seventh roots of 0^+ symmetry is quite large. All important $A0^+$ components appear in the seventh root of the 0^+ symmetry. The equilibrium bond length of $A0^+$ is estimated to be 3.07 Å after fitting the adiabatic curve. The $A0^+$ component is characterized dominantly by the $A^3\Pi$ state around r_e. Some of these high-lying 0^+ states may become important due to their transitions to the ground-state component $X^3\Sigma^-_{0^+}$. However, none of these 0^+ states of TlX have been experimentally observed.

B. TlSb. Spectroscopic constants, including dissociation energies (D_e) of at least twelve low-lying Ω states of TlSb within 21 000 cm^{-1}, are given in Table 9. The zero-field splitting

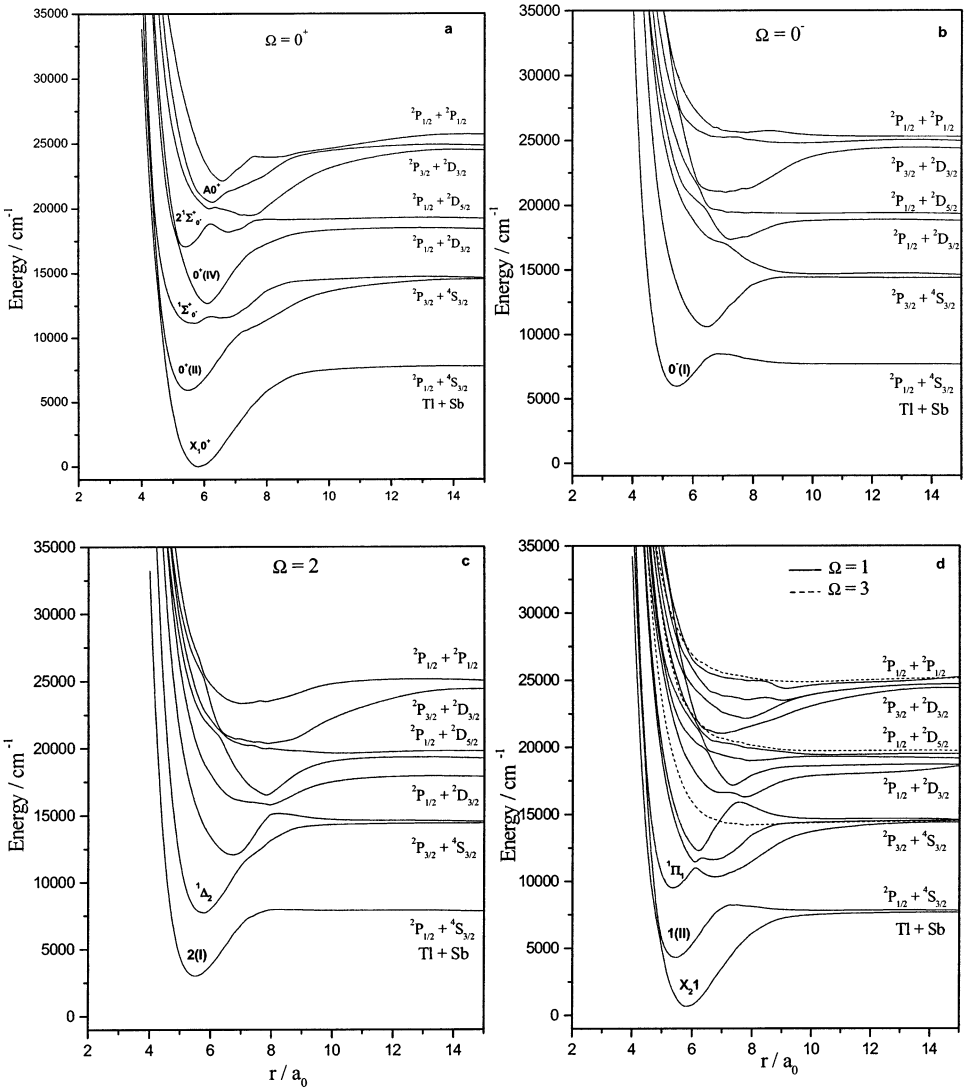

Figure 5. Computed potential energy curves of low-lying Ω states of TlSb for (a) $\Omega = 0^+$, (b) $\Omega = 0^-$, (c) $\Omega = 2$, and (d) $\Omega = 1, 3$.

TABLE 9: Spectroscopic Constants of Low-Lying Ω States of TlSb

state	T_e/cm^{-1}	r_e/Å	ω_e/cm^{-1}	D_e/eV
$X_1 0^+$	0	3.08	113	0.95
$X_2 1$	639	3.09	112	0.87
2(I)	2955	2.91	119	0.58
1(II)	4255	2.89	123	0.42
0^+(II)	5895	2.90	123	1.06
0^-(I)	5921	2.89	125	1.05
$^1\Delta_2$	7695	3.03	123	0.83
$^1\Pi_1$	9453	2.84	135	0.62
$^1\Sigma^+_{0^+}$	11 127	2.96	91	0.41
0^+(IV)	12 837	3.22	119	0.67
$2^1\Sigma^+_{0^+}$	17 002	2.87	152	0.29
$A0^+$	20 642	3.28	94	0.49

($X_2 1 - X_1 0^+$) of the ground state of this molecule is calculated to be 639 cm^{-1}, which is expectedly larger than that of TlAs. Spectroscopic constants of both the components of $X^3\Sigma^-$ remain almost the same as those of the pure Λ-S state. The spin−orbit components of the first excited state ($^3\Pi$) split in the inverted order. The largest spin−orbit splitting of the $^3\Pi$ state is estimated to be 2966 cm^{-1}. Four spin components of the $^3\Pi$ state of TlSb in the Franck−Condon region are designated as 2(I), 1(II), 0^+(II), and 0^-(I). Spectroscopic constants of these components obtained from the adiabatic potential curves are given in Table 9. Potential energy curves of some of the low-lying 0^+, 0^-, 1, 2, and 3 components are shown in Figure 5a−d. In the shorter bond length region, curves of 0^+(II) and 1(II) components have many avoided crossings with the corresponding ground-state components. The nature of these components at longer bond distances is somewhat complicated. Both $^1\Delta_2$ and $^1\Pi_1$ components are not much perturbed by the spin−orbit coupling except the increase in the transition energy by 1150 and 1650 cm^{-1}, respectively. A minimum in the potential curve of the 0^-(II) state appears due to a strong avoided crossing between the repulsive $^5\Pi_{0^-}$ and bound 0^-(I)($^3\Pi$) curves. The $^1\Sigma^+_{0^+}$ component undergoes several avoided crossings, hence the adiabatic curve of $^1\Sigma^+_{0^+}$ in Figure 5a looks shallow. Spectroscopic parameters computed from the diabatic curve of $^1\Sigma^+_{0^+}$ are reported in Table 9. The potential curve of 2(III) in Figure 5c shows a very shallow minimum around 7.0 a_0 due to an avoided crossing between $^1\Delta_2$ and $^5\Pi_2$ components. Similarly, the fourth root of 0^+ shows a potential minimum which arises from another avoided crossing. Fitting the adiabatic curve of 0^+(IV), the minimum is located at 3.22 Å with ω_e=119 cm^{-1}.

The 0^+ component of $2^1\Sigma^+$ is the fifth root of this symmetry, and it has a minimum around 2.87 Å with ω_e=152 cm^{-1} in the diabatic curve. In the potential curve of $2^1\Sigma^+_{0^+}$, there are several avoided crossings beyond 6.2 a_0. The estimated transition energy

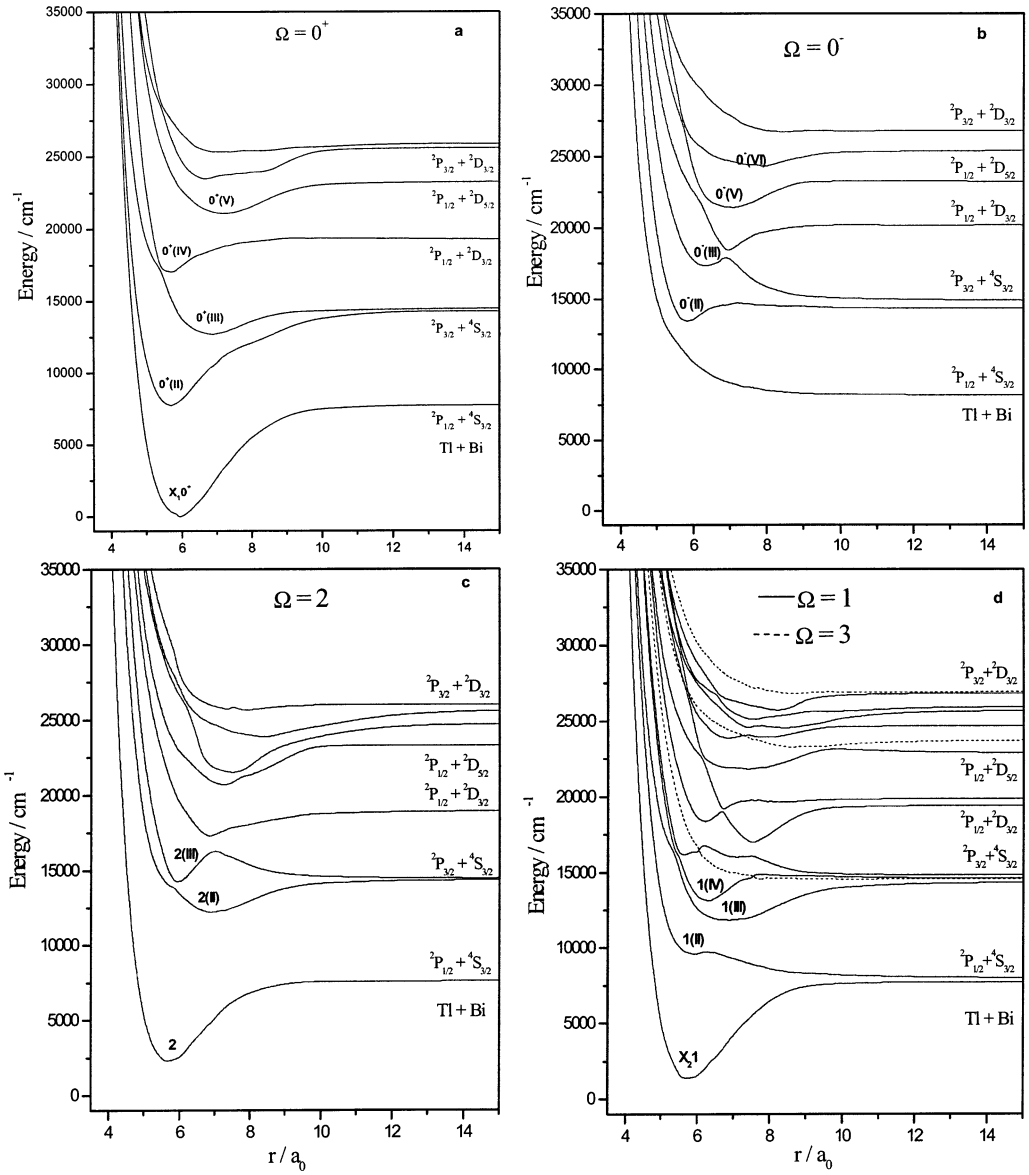

Figure 6. Computed potential energy curves of low-lying Ω states of TlBi for (a) Ω = 0^+, (b) Ω = 0^-, (c) Ω = 2, and (d) Ω = 1, 3.

of $2^1\Sigma_{0^+}^+$ is about 17 000 cm^{-1}. Both 0^+(IV) and $2^1\Sigma_{0^+}^+$ states may be suitable for transitions to the ground-state component. Around the potential minimum, the 0^+(VII) component has a substantial contribution of $3^3\Pi$, while in the shorter bond length region, the $2^3\Pi$ state dominates. Hence, the 0^+(VII) state is designated as $A0^+$, analogous to the $A0^+$ state of TlAs. It may be recalled that the $3^3\Pi$ state of TlSb is not bound but the $A0^+$ component is. The adiabatic transition energy of $A0^+$ is about 20 642 cm^{-1} with r_e=3.28 Å and ω_e=94 cm^{-1}. The next higher root, 0^+(VIII) is characterized by $2^3\Sigma^-$ in the Franck−Condon region of the potential curve. Two avoided crossings near 6.7 and 8.0 a_0 are seen in the potential curve of this root.

C. TlBi. Potential energy curves of low-lying Ω states of TlBi are shown in Figure 6a−d, while the estimated spectroscopic constants are given in Table 10. The zero-field splitting of the ground state of TlBi is quite large (∼1285 cm^{-1}), with X_10^+ lying lower than X_21. The computed equilibrium bond length of X_21 is shorter than that of the X_10^+ component by about 0.06 Å. The overall spin−orbit mixing is quite strong, as noted in the composition of the wave function. The ground-state component consists of 64% $X^3\Sigma^-$, 16%$^1\Sigma^+$, and 8% $^5\Pi$ at r_e. Similarly, the $^3\Pi_1$ component participates strongly (22%) in the X_21 state at the equilibrium bond length. The second root of 0^+ is dominated by the $^3\Pi_{0^+}$ component and its transition energy is about 7700 cm^{-1}, which is shifted considerably due to the spin−orbit coupling. The lowest Ω = 2 state is characterized mainly by $^3\Pi_2$, and it lies much below the other components of $^3\Pi$. There is an avoided crossing between the 0^- components of $^3\Pi$ and $^5\Pi$ around 5.5 a_0 (Figure 6b). The

TABLE 10: Spectroscopic Constants of Low-Lying Ω States of TlBi

state	T_e/cm^{-1}	r_e/Å	ω_e/cm^{-1}	D_e/eV
X_10^+	0	3.12	94	0.97
X_21	1285	3.06	99	0.81
2(I)	2208	3.01	98	0.69
0^+(II)	7700	3.00	102	0.85
1(II)	9538	3.13	63	
1(III)	11 759	3.64	40	0.34
2(II)	12 170	3.67	48	0.29
0^+(III)	12 637	3.62	52	0.23
1(IV)	13 058	3.32	89	0.18
0^-(II)	13 324	3.09	117	0.15
2(III)	13 874	3.06	106	0.08
0^+(IV)	16 989	2.98	92	0.31
0^-(III)	17 246	3.35	82	
0^+(V)	21 020	3.80	44	0.33
0^-(V)	21 339	3.70	55	0.29

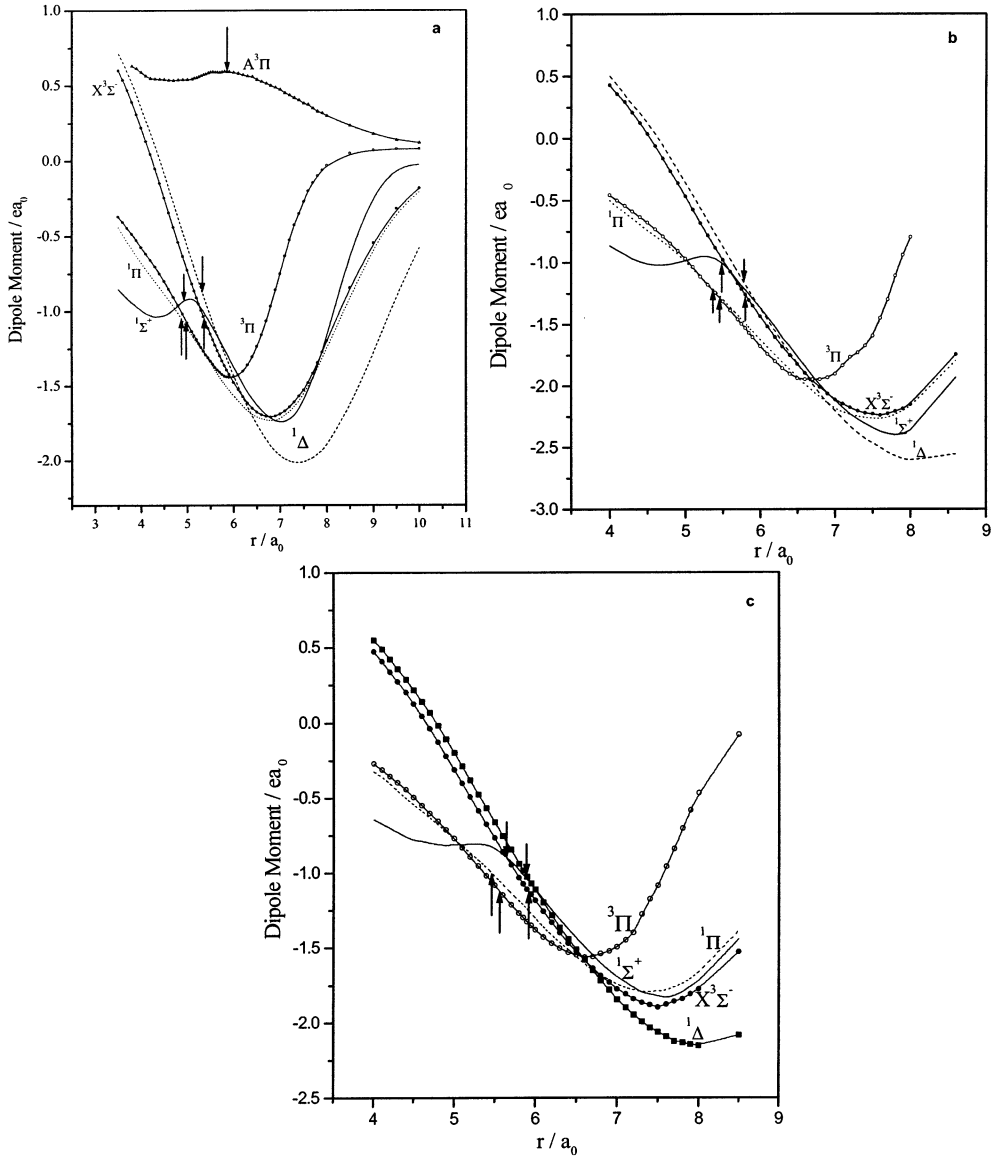

Figure 7. Dipole moment functions of a few states of (a) TlAs, (b) TlSb, and (c) TlBi (arrows correspond to the equilibrium bond lengths).

transition energy of 0^-(II) estimated from the adiabatic curve is 13 324 cm^{-1}. The state originates mainly from $^3\Pi$, but the participation of the $^5\Pi_{0^-}$ component is more than 20% in the Franck−Condon region. The largest splitting between the 2(I) and 0^-(II) components of $^3\Pi$ is calculated to be about 11 116 cm^{-1}. Although the $^5\Pi$ state is repulsive, some of its spin components, such as 0^+(III), 2(II), 1(III), and 1(IV), have shown shallow potential minima due to the spin−orbit coupling. The vibrational frequencies of these states are quite small and the equilibrium bond lengths are quite large. The composition of 1(IV) varies considerably as a function of bond length. Because of the spin−orbit coupling, the transition energy of 2(III), which is dominated by the $^1\Delta$ state, is increased by about 8000 cm^{-1}. The interaction between $^1\Delta_2$ and $^3\Pi_2$ components around the bond length of 6.0 a_0 is quite large, and the avoided crossing in this region is noted in Figure 6c. The only spin component of $^1\Pi$ undergoes several avoided crossings. The higher roots of $\Omega = 1$ are complex in nature.

The composition of the fourth root of 0^+ is relatively less complex. An avoided crossing around 5.6 a_0 between the third and fourth root is shown in Figure 6a. The transition energy of 0^+(IV) from the adiabatic curve is estimated to be 16 989 cm^{-1} with r_e=2.98 Å and ω_e=92 cm^{-1}, and the component is dominated by the $^1\Sigma^+$ state. The fifth root of 0^+ has a shallow potential minimum at a large bond length. The computed transition energy of 0^+(V) is about 21 020 cm^{-1} with r_e=3.8 Å and ω_e=44 cm^{-1}. There exists a minimum in the potential curve of 0^-(III) at 3.35 Å with a binding energy of only 500 cm^{-1}. The fifth root of the 0^- symmetry has a potential minimum around 3.7 Å with different compositions at different bond lengths. Figure 6c shows the overall feature of the higher roots of $\Omega = 2$, which are not so important to mention here. The eighth root of $\Omega = 1$ has also a shallow potential well, as shown in Figure 6d.

The calculated D_e's of the Ω states of TlBi are also reported in Table 10. The potential curve of 1(II) consists of only one vibrational level, and it predissociates to the lowest dissociation limit, $^2P_{1/2}$(Tl) + $^4S_{3/2}$(Bi), with a small barrier (Figure 6d). On the other hand, the 0^-(III) state has six vibrational levels in its potential curve, and hence, it has to cross a larger barrier before dissociating to the second limit.

V. Dipole Moments, Transition Dipole Moments, and Radiative Lifetimes of Excited States

Dipole moments (μ_e) of the ground and some low-lying states of TlX at r_e computed from the MRDCI wave functions are

TABLE 11: Dipole Moments (D) of Low-Lying States of TlX (X=As, Sb, Bi) at r_e

	dipole moment (μ_e)		
state	TlAs	TlSb	TlBi
$X^3\Sigma^-$	−2.66	−3.27	−2.89
$X_1 0^+$	−2.35	−2.91	−2.25
$^3\Pi$	−2.71	−3.29	−2.87
$^1\Sigma^+$	−2.37	−2.63	−2.27
$^1\Delta$	−2.20	−2.93	−2.57
$^1\Pi$	−2.68	−3.08	−2.57
$A^3\Pi$	1.51		

TABLE 12: Radiative Lifetimes (s) of Some Excited States of TlAs at the Lowest Three Vibrational Levels[a]

	lifetime of the upper state			total lifetime of the upper state at
transition	$v'=0$	$v'=1$	$v'=2$	$v'=0$
$A^3\Pi$-$X^3\Sigma^-$	1.49(−6)	1.50(−6)	1.52(−6)	
$A^3\Pi$-$^3\Pi$	3.10(−6)	3.19(−6)	3.26(−6)	
$A^3\Pi-2^3\Pi$	2.05(−4)	1.84(−4)	1.67(−4)	$\tau(A^3\Pi) = 1.00(-6)$
$2^1\Sigma^+$-$^1\Pi$	6.73(−6)	6.75(−6)	6.76(−6)	
$2^1\Sigma^+$-$^1\Sigma^+$	1.48(−5)	1.48(−5)	1.47(−5)	$\tau(2^1\Sigma^+) = 4.63(-6)$
$A0^+$-$X_1 0^+$	7.60(−5)	7.40(−5)	1.06(−4)	
$A0^+$-$X_2 1$	6.65(−6)	6.35(−6)	6.05(−6)	
$A0^+-0^+$(II)	6.80(−6)	3.60(−6)	4.20(−6)	
$A0^+-1$(II)	2.90(−3)	4.60(−3)	1.20(−2)	$\tau(A0^+) = 3.22(-6)$
$2^1\Sigma^+_{0^+}$-$^1\Sigma^+_{0^+}$	1.52(−5)	1.57(−5)	1.70(−5)	
$2^1\Sigma^+_{0^+}$-$X_1 0^+$	8.64(−5)	1.17(−4)	1.04(−4)	
$2^1\Sigma^+_{0^+}-0^+$(II)	2.20(−4)	3.50(−4)	2.60(−4)	$\tau(2^1\Sigma^+_{0^+}) = 1.22(-5)$
$^1\Sigma^+_{0^+}$-$X_1 0^+$	1.41(−3)	1.95(−3)	2.57(−3)	
$^1\Sigma^+_{0^+}$-$X_2 1$	1.79(−3)	1.87(−3)	1.88(−3)	$\tau(^1\Sigma^+_{0^+}) = 7.90(-4)$
0^+(II)-$X_1 0^+$	1.42(−2)	4.97(−3)	3.21(−3)	
0^+(II)-$X_2 1$	2.50(−4)	2.50(−4)	2.40(−4)	$\tau(0^+(\text{II})) = 2.50(-4)$

[a] Values in parentheses are the powers to the base 10.

displayed in Table 11. Parts a−c of Figure 7 show the dipole moment functions of three molecules in $X^3\Sigma^-$, $^3\Pi$, $^1\Pi$, $^1\Delta$, and $^1\Sigma^+$ states. The dipole-moment curve of the $A^3\Pi$ state of TlAs is also plotted in Figure 7a. Except for $A^3\Pi$, μ_e values of all states are negative, indicating Tl^+X^- polarity. The ground-state dipole moment of TlAs, TlSb, and TlBi are estimated to be −2.66, −3.27, and −2.89 D, respectively, while after the inclusion of the spin−orbit coupling the respective values of the ground-state component ($X_1 0^+$) decrease to −2.35, −2.91, and −2.25 D. Such a lowering of the dipole moment due to the spin−orbit coupling can be attributed to the change of ionization potential and electron affinity associated with the spin−orbit splitting. The $A^3\Pi$ state of TlAs shows the opposite polarity throughout the curve with a dipole moment of 1.51 D at r_e, and the dipole moment function is slowly varying. All the dipole curves are smooth and tend to zero in the longer bond length region. Most of the curves have an extremum. The first excited state ($^3\Pi$) of each of three molecules has a dipole moment comparable with that of the ground state.

A. TlAs. Three transitions from $A^3\Pi$ to $X^3\Sigma^-$, $^3\Pi$, and $2^3\Pi$ states of TlAs are computed from the Λ-S CI wave functions. The $A^3\Pi-2^3\Pi$ transition is less probable, as evident from the partial lifetime for the transition as shown in Table 12. Summing up transition probabilities of these transitions, the total radiative lifetime of $A^3\Pi$ is estimated to be 1.0 μs. Two transitions such as $2^1\Sigma^+-^1\Pi$ and $2^1\Sigma^+-^1\Sigma^+$ are also studied here. The former transition is expected to be twice as strong as the later one. The $2^1\Sigma^+$ state is more than four times longer-lived than $A^3\Pi$. Transition-dipole-moment functions of the above-mentioned transitions are shown in Figure 8a. All the transition-moment curves are smooth. The transition-moment value of the $A^3\Pi-X^3\Sigma^-$ transition near 4.2 a_0 is about 0.57 ea_0 for TlAs. Table 12 also shows the partial and total radiative lifetimes of some spin−orbit states of TlAs. The 0^+ component of $A^3\Pi$ undergoes four transitions, such as $A0^+$-$X_1 0^+$, $A0^+$-$X_2 1$, $A0^+$-0^+(II), and $A0^+$-1(II). The last one is much weaker than the remaining three. Transitions from the $2^1\Sigma^+_{0^+}$ component to the lowest three 0^+ components are also studied. The $2^1\Sigma^+_{0^+}-0^+$(II) transition is comparatively weak and the partial lifetime for this transition is of the order of 20 ms. Transitions from $^1\Sigma^+_{0^+}$ to both the components of $X^3\Sigma^-$ should have comparable intensities. Two weak transitions, such as $0^+(\text{II})-X_1 0^+$ and $0^+(\text{II})-X_2 1$ are possible. The computed total radiative lifetime of 0^+(II) is found to be 0.25 ms at $v' = 0$.

TABLE 13: Radiative Lifetimes (s) of Some Excited States of TlSb at the Lowest Three Vibrational Levels[a]

	lifetime of the upper state			total lifetime of the upper state at
transition	$v'=0$	$v'=1$	$v'=2$	$v'=0$
$2^1\Sigma^+$-$^1\Pi$	1.11(−5)	1.12(−5)	1.13(−5)	
$2^1\Sigma^+$-$^1\Sigma^+$	1.90(−5)	1.86(−5)	1.85(−5)	$\tau(2^1\Sigma^+) = 7.01(-6)$
$A0^+$-$X_1 0^+$	2.27(−4)	3.01(−4)	7.91(−4)	
$A0^+$-$X_2 1$	1.65(−4)	7.60(−5)	5.30(−5)	$\tau(A0^+) = 9.56(-5)$
$2^1\Sigma^+_{0^+}$-$^1\Pi_1$	1.19(−5)	1.20(−5)	1.21(−5)	
$2^1\Sigma^+_{0^+}$-$^1\Sigma^+_{0^+}$	1.92(−5)	1.94(−5)	2.79(−5)	
$2^1\Sigma^+_{0^+}$-$X_1 0^+$	3.60(−4)	7.40(−4)	3.30(−4)	
$2^1\Sigma^+_{0^+}-0^+$(II)	2.02(−3)	1.26(−3)	6.54(−4)	
$2^1\Sigma^+_{0^+}$-$X_2 1$	1.39(−2)	2.33(−3)	8.35(−4)	$\tau(2^1\Sigma^+_{0^+}) = 7.18(-6)$
0^+(II)-$X_1 0^+$	1.07(−4)	1.02(−4)	8.80(−5)	
0^+(II)-$X_2 1$	2.20(−4)	2.24(−4)	2.30(−4)	$\tau(0^+(\text{II})) = 7.20(-5)$
$^1\Sigma^+_{0^+}$-$X_1 0^+$	3.10(−4)	1.33(−4)	7.10(−5)	
$^1\Sigma^+_{0^+}$-$X_2 1$	5.61(−4)	7.75(−4)	7.75(−4)	
$^1\Sigma^+_{0^+}-0^+$(II)	6.82(−4)	8.12(−4)	9.94(−4)	$\tau(^1\Sigma^+_{0^+}) = 1.54(-4)$

[a] Values in parentheses are the powers to the base 10.

B. TlSb. At the Λ-S level, only $2^1\Sigma^+-^1\Sigma^+$ and $2^1\Sigma^+-^1\Pi$ transitions are computed for the TlSb molecule. The transition-dipole-moment curves of these transitions are found to be smooth, as shown in Figure 8b. The transition-moment curve of the $2^1\Sigma^+-^1\Sigma^+$ transition shows a sharp peak near 5.3 a_0. The partial radiative lifetimes for these two transitions are of comparable magnitude. Table 13 shows the computed partial and total radiative lifetimes of $2^1\Sigma^+$, along with those of some Ω components. The total lifetime of the $2^1\Sigma^+$ state in the absence of any spin−orbit coupling is of the order of 7 μs at the lowest vibrational level. The inclusion of the spin−orbit coupling increases the lifetime of the $2^1\Sigma^+_{0^+}$ component only marginally. Transition moments of five transitions from $2^1\Sigma^+_{0^+}$ to $^1\Pi_1$, $^1\Sigma^+_{0^+}$, $X_1 0^+$, $X_2 1$, and 0^+(II) are computed from the MRDCI wave functions. As expected, first two transitions are stronger than the remaining ones. Transitions from 0^+(II) to both components of the ground states are not very strong. At the lowest vibrational level ($v' = 0$), the lifetime of 0^+(II) is within 100 μs. The spin-forbidden transitions from the $^1\Sigma^+_{0^+}$ component to $X_1 0^+$, $X_2 1$, and 0^+(II) are expectedly weak.

C. TlBi. Figure 8c shows the transition-dipole-moment functions of $2^1\Sigma^+-^1\Pi$ and $2^1\Sigma^+-^1\Sigma^+$ transitions of TlBi. All the dipole curves are smooth and comparable with those of TlSb. The radiative lifetimes for these two transitions, as well as other spin-included transitions, are given in Table 14. The partial lifetime of $2^1\Sigma^+-^1\Sigma^+$ at the lowest vibrational level is twice that of $2^1\Sigma^+-^1\Pi$. The 0^+(II) state, which is dominated by $^3\Pi_0{}^+$, has a total radiative lifetime of 8.2 μs. The $0^+(\text{II})-X_1 0^+$ transition is predicted to be much stronger than $0^+(\text{II})-X_2 1$. The 0^+(IV) component is associated with four transitions of which $0^+(\text{IV})-1(\text{II})$ is much weaker than the others. The total radiative lifetime of 0^+(IV) at $v' = 0$ is about 7.52 μs. Two

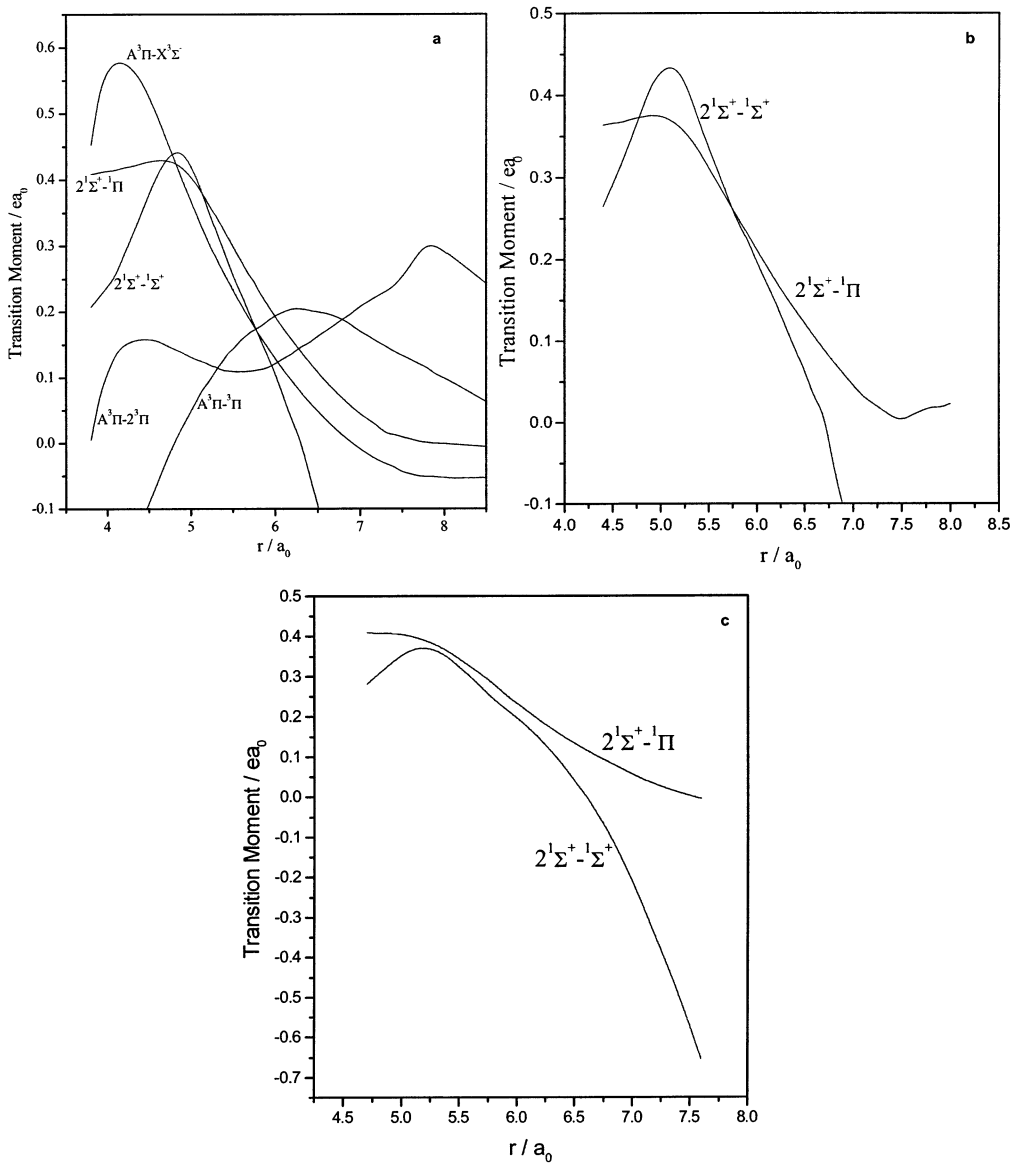

Figure 8. Transition-moment functions of some important transitions in (a) TlAs, (b) TlSb, and (c) TlBi.

TABLE 14: Radiative Lifetimes (s) of Some Excited States of TlBi at the Lowest Three Vibrational Levels[a]

transition	lifetime of the upper state $v'=0$	$v'=1$	$v'=2$	total lifetime of the upper state at $v'=0$
$2^1\Sigma^+$-$^1\Pi$	1.04(−5)	1.04(−5)	1.05(−5)	
$2^1\Sigma^+$-$^1\Sigma^+$	2.04(−5)	2.05(−5)	2.06(−5)	$\tau(2^1\Sigma^+) = 6.89(-6)$
0^+(II)-X_10^+	8.96(−6)	8.68(−6)	8.34(−6)	
0^+(II)-X_21	9.70(−5)	9.80(−5)	1.00(−4)	$\tau(0^+(\text{II})) = 8.20(-6)$
0^+(IV)-X_21	1.25(−5)	1.36(−5)	1.54(−5)	
0^+(IV)−0^+(II)	3.71(−5)	5.20(−5)	7.57(−5)	
0^+(IV)-X_10^+	3.93(−5)	1.67(−5)	8.67(−6)	
0^+(IV)−1(II)	1.65(−3)	2.17(−3)	6.47(−3)	$\tau(0^+(\text{IV})) = 7.52(-6)$
1(II)-X_21	1.25(−5)	1.31(−5)		
1(II)-X_10^+	1.78(−5)	1.90(−5)		$\tau(1(\text{II})) = 7.34(-6)$
X_21-X_10^+	4.91(−2)	5.02(−2)	5.15(−2)	$\tau(X_21) = 4.91(-2)$

[a] Values in parentheses are the powers to the base 10.

transitions from 1(II), which is dominated by the $^3\Pi_1$ component, are expected to be of almost the same intensities. The estimated lifetime of 1(II) is about 7.3 μs.

Transition-dipole-moment values for transitions which connect the ground-state component (X_10^+) and other excited Ω states at the ground-state r_e are tabulated in Table 15. These data may be quite useful for the experimental studies of TlX molecules.

TABLE 15: Transition Dipole Moments for Transitions between the Ground-State Component and Other Ω States at the Ground-State r_e

molecule	transition	transition moment/ea_0
TlAs	$A0^+-X_10^+$	0.0373
	$2^1\Sigma_{0^+}^+-X_10^+$	0.0452
	$^1\Sigma_{0^+}^+-X_10^+$	0.0044
	0^+(II)$-X_10^+$	0.0851
TlSb	$A0^+-X_10^+$	0.00037
	$2^1\Sigma_{0^+}^+-X_10^+$	0.0306
	0^+(II)$-X_10^+$	0.2385
	$^1\Sigma_{0^+}^+-X_10^+$	0.0776
TlBi	0^+(II)$-X_10^+$	0.4084
	0^+(IV)$-X_10^+$	0.0949
	$1(\text{II})-X_10^+$	0.1799
	$X_21-X_10^+$	0.0621

VI. Effects of d Correlations on the Spectroscopic Parameters

Additional CI calculations that include 20 d electrons of Tl and X are carried out. We have computed only the lowest root in each irreducible representation. The configuration-selection threshold has been kept at the same value as that used in the

TABLE 16: Spectroscopic Constants of Some Low-Lying States of TlX (X = As, Sb, Bi) Including 20 d electrons

molecule	state	T_e/cm^{-1}	r_e/Å	ω_e/cm^{-1}	D_e/eV
TlAs	$X^3\Sigma^-$	0	2.84	156	1.31
	$^3\Pi$	2237	2.59	178	
	$^1\Pi$	7376	2.58	190	
	$^1\Delta$	8458	2.81	158	
	$^1\Sigma^+$	10 050	2.55	154	
TlSb	$X^3\Sigma^-$	0	3.12	108	1.22
	$^3\Pi$	2286	2.83	130	
	$^1\Delta$	6530	3.06	124	
	$^1\Pi$	6717	2.80	141	
	$^1\Sigma^+$	8650	2.98	118	
TlBi	$X^3\Sigma^-$	0	3.12	102	1.13
	$^3\Pi$	2151	2.90	130	
	$^1\Delta$	7109	3.10	105	
	$^1\Pi$	7362	2.90	115	
	$^1\Sigma^+$	9656	3.02	87	

calculations without d electrons. Table 16 displays r_e, ω_e, and T_e values of five low-lying states of all three thallium isomers with d electrons in the calculations. The ground-state properties of TlAs do not change at all, while for TlSb the bond length is increased by 0.04 Å and for TlBi it is reduced by 0.02 Å. The bond length of the first excited state ($^3\Pi$) is shortened by 0.04−0.05 Å due to d correlation, while its transition energy is reduced by 200−1000 cm^{-1}. The largest change is found in TlSb. Transition energies of $^1\Pi$ for all three isomers are decreased by almost the same amount as those in $^3\Pi$ states. The spectroscopic constants of $^1\Delta$ in TlSb remain unchanged. However, for TlAs and TlBi molecules, transition energies of this state are reduced by 629 and 1138 cm^{-1}, respectively. The inclusion of d electrons has enhanced the transition energy of $^1\Sigma^+$ in TlAs and TlBi by 600−800 cm^{-1}, while for the TlBi molecule, it is reduced by about 700 cm^{-1}. The ground-state dissociation energies of all these molecules are increased by d-electron correlation.

VII. Concluding Remarks

The electronic states and spectroscopic feature of TlX (X = As, Sb, Bi) molecules are computed by using ab initio based MRDCI calculations. Neither experimental nor theoretical studies of these molecules are performed as yet. The ground state of TlX belongs to the $X^3\Sigma^-$ symmetry like all other group III−V molecules. The r_e, ω_e, and D_e values of the ground state show an expected trend with the mass of the molecule. The ground-state dissociation energies follow the trend: D_e(TlAs) > D_e(TlSb) > D_e(TlBi). The changes in the spectroscopic constants due to the d-electron correlation are small. For all three molecules, the X_10^+ ($^3\Sigma^-$) component lies lower than X_21 ($^3\Sigma^-$). The zero-field splitting for the TlBi molecule is as large as 1285 cm^{-1}, which shows a strong spin−orbit coupling. The dissociation energy of the ground-state component (X_10^+) is about 1 eV for each of these three molecules. The spin−orbit coupling reduces the absolute value of μ_e for TlBi more than for the other two molecules. The potential energy curves of Ω states of TlBi are quite complex and there are many avoided crossings. The third root of the $^3\Pi$ symmetry has a potential minimum only for the TlAs molecule and it disappears for the heavier isomers. In general, this root has been found to be significant in other group III−V diatomic molecules, as it undergoes a strong transition to the ground state. Transition-dipole-moment functions for the low-lying transitions are smooth. The $A^3\Pi$ state of TlAs is found to be short-lived, with a radiative lifetime of about 1 μs. After the inclusion of spin−orbit coupling, the lifetime of the $A0^+$ component of TlAs is increased by three times. However, this particular state of heavier molecules is very weakly bound.

Acknowledgment. We thank Prof. Dr. Robert J. Buenker, Wuppertal, Germany for making available the MRDCI codes.

References and Notes

(1) O'Brien, S. C.; Liu, Y.; Zhang, Q.; Heath, J. R.; Tittel, F. K.; Curl, R. F.; Smalley, R. E. *J. Chem. Phys.* **1986**, *84*, 4074.
(2) Liu, Y.; Zhang, Q.; Tittel, F. K.; Curl, R. F.; Smalley, R. E. *J. Chem. Phys.* **1986**, *85*, 7434.
(3) Zhang, Q.; Liu, Y.; Curl, R. F.; Tittel, F. K.; Smalley, R. E. *J. Chem. Phys.* **1988**, *88*, 1670.
(4) Wang, L.; Chibante, L. P. F.; Tittel, F. K.; Curl, R. F.; Smalley, R. E. *Chem. Phys. Lett.* **1990**, *172*, 335.
(5) Jin, C.; Taylor, K.; Conciecao, J.; Smalley, R. E. *Chem. Phys. Lett.* **1990**, *175*, 17.
(6) Lou, L.; Wang, L.; Chibante, L. P. F.; Laaksonen, R. T.; Nordlanden, P.; Smalley, R. E. *J. Chem. Phys.* **1991**, *94*, 8015.
(7) Lemire, G. W.; Bishea, G. A.; Heidecke, S. A.; Morse, M. D. *J. Chem. Phys.* **1990**, *92*, 121.
(8) Li, S.; Van Zee, R. J.; Weltner, W., Jr. *J. Phys. Chem.* **1993**, *97*, 11393.
(9) Van Zee, R. J.; Li, S.; Weltner, W., Jr. *J. Chem. Phys.* **1993**, *98*, 4335.
(10) Li, S.; Van Zee, R. J.; Weltner, W., Jr. *J. Phys. Chem.* **1994**, *98*, 2275.
(11) Piacente, V.; Malaspina, L. *J. Chem. Phys.* **1972**, *56*, 1780.
(12) Balducci, G.; Ferro, D.; Piacente, V. *High Temp. Sci.* **1981**, *14*, 207.
(13) Piacente, V.; Balducci, G. *Adv. Mass Spectrom.* **1978**, *7A*, 626.
(14) De Maria, G.; Malaspina, L.; Piacente, V. *J. Chem. Phys.* **1972**, *56*, 1978.
(15) Manna, B.; Das, K. K. *J. Phys. Chem. A* **1998**, *102*, 9876.
(16) Manna, B.; Das, K. K. *J. Mol. Struct.: THEOCHEM* **1999**, *467*, 135.
(17) Manna, B.; Dutta, A.; Das, K. K. *J. Phys. Chem. A* **2000**, *104*, 2764.
(18) Manna, B.; Dutta, A.; Das, K. K. *J. Mol. Struct.: THEOCHEM* **2000**, *497*, 123.
(19) Dutta, A.; Chattopadhyay, A.; Das, K. K. *J. Phys. Chem. A* **2000**, *104*, 9777.
(20) Dutta, A.; Giri, D.; Das, K. K. *J. Phys. Chem. A* **2001**, *105*, 9049.
(21) Chattopadhyay, A.; Chattopadhyaya, S.; Das, K. K. *J. Phys. Chem. A* **2002**, *106*, 9049.
(22) Chattopadhyay, A.; Chattopadhyaya, S.; Das, K. K. *J. Mol. Struct.: THEOCHEM* **2003**, *625*, 95.
(23) Wildman, S. A.; Dilabio, G. A.; Christiansen, P. A. *J. Chem. Phys.* **1997**, *107*, 9975.
(24) Hurley, M. M.; Pacios, L. F.; Christiansen, P. A. *J. Chem. Phys.* **1986**, *84*, 6840.
(25) LaJohn, L. A.; Christiansen, P. A.; Ross, R. B.; Atashroo, T.; Ermler, W. C. *J. Chem. Phys.* **1987**, *87*, 2812.
(26) Alekseyev, A. B.; Liebermann, H.-P.; Hirsch, G.; Buenker, R. J. *J. Chem. Phys.* **1998**, *108*, 2028.
(27) Alekseyev, A. B.; Liebermann, H.-P.; Lingott, R. M.; Bludský, O.; Buenker, R. J. *J. Chem. Phys.* **1998**, *108*, 7695.
(28) Balasubramanian, K. *J. Chem. Phys.* **1989**, *91*, 2443.
(29) Lingott, R. M.; Liebermann, H.-P.; Alekseyev, A. B.; Buenker, R. J. *J. Chem. Phys.* **1999**, *110*, 11294.
(30) Buenker, R. J.; Peyerimhoff, S. D. *Theor. Chim. Acta* **1974**, *35*, 33.
(31) Buenker, R. J.; Peyerimhoff, S. D. *Theor. Chim. Acta* **1975**, *39*, 217.
(32) Buenker, R. J. *Int. J. Quantum Chem.* **1986**, *29*, 435.
(33) Buenker, R. J.; Peyerimhoff, S. D.; Butcher, W. *Mol. Phys.* **1978**, *35*, 771.
(34) Buenker, R. J.; In *Proceedings of the Workshop on Quantum Chemistry and Molecular Physics;* Burton, P., Ed.; University Wollongong: Wollongong, Australia; 1980; *Studies in Physical and Theoretical Chemistry*; Carbó, R., Ed.; Current Aspects of Quantum Chemistry 21; Elsevier: Amsterdam, 1981.
(35) Buenker, R. J.; Phillips, R. A. *J. Mol. Struct.: THEOCHEM* **1985**, *123*, 291.
(36) Davidson, E. R. In *The World of Quantum Chemistry*; Daudel, R., Pullman, B., Eds.; Reidel: Dordrecht, 1974.
(37) Hirsch, G.; Bruna, P. J.; Peyerimhoff, S. D.; Buenker, R. J. *Chem. Phys. Lett.* **1977**, *52*, 442.
(38) Alekseyev, A. B.; Buenker, R. J.; Liebermann, H.-P.; Hirsch, G. *J. Chem. Phys.* **1994**, *100*, 2989.
(39) Cooley, J. W. *Math. Comput.* **1961**, *15*, 363.
(40) Moore, C. E. *Atomic Energy Levels*; National Bureau of Standards: Washington, DC., 1971; Vol. 3.